Substrate Requirements for SPPL2b-dependent Regulated Intramembrane Proteolysis*[S]

Lucas Martin[1], **Regina Fluhrer**[2], and **Christian Haass**[3]

From the Center for Integrated Protein Science Munich and Adolf-Butenandt-Institute, Department of Biochemistry, Laboratory for Neurodegenerative Disease Research, Ludwig-Maximilians-University, 80336 Munich, Germany

Intramembrane proteolysis is now widely recognized as an important physiological pathway required for reverse signaling and membrane protein degradation. Aspartyl intramembrane cleaving proteases of the GXGD-type play an important regulatory role in health and disease. Besides γ-secretase/presenilin, signal peptide peptidase (SPP) and SPP-like (SPPL) peptidases also belong to the family of GXGD-type aspartyl proteases. Although recently the first SPPL2a/b substrates have been identified, very little is known about substrate requirements, which allow them to be efficiently processed within the membrane. We demonstrate that similar to γ-secretase substrates, intramembrane proteolysis of Bri2 (Itm2b) is greatly facilitated by an initial shedding event mediated by ADAM-10. Serial deletions revealed that the length of the ectodomain negatively correlates with efficient intramembrane proteolysis. Bri3 (Itm2c), which is highly homologous to Bri2, fails to be shed. Failure of shedding of Bri3 is accompanied by a lack of intramembrane proteolysis by SPPL2b. Surprisingly, a low molecular weight membrane-retained stub of Bri3 also fails to be processed by SPPL2b, indicating that shedding *per se* is not sufficient for subsequent intramembrane proteolysis. Extensive domain swapping analysis reveals that primary sequence determinants within the intracellular domain and the transmembrane domain together with short luminal juxtamembrane sequences are required for efficient intramembrane proteolysis.

Signal peptide peptidase (SPP)[4] (1), its homologues, the SPP-like peptidases (SPPL) SPPL2a, b, and c and SPPL3 (2, 3) as well as the Alzheimer's disease-associated presenilins (PS1 or PS2) are intramembrane-cleaving proteases (ICLiPs) of the GXGD-type aspartyl protease family (4, 5). GXGD designates a novel active site motif located within transmembrane domain (TMD) 7 of all known intramembrane-cleaving aspartyl proteases (6). The GXGD motif contains one of the two critical aspartyl residues conserved in all GXGD-type proteases. The second aspartyl residue is part of a conserved YD motif located in TMD 6. Both motifs share no homologies with conventional aspartyl proteases (6). SPP/SPPLs and PSs only share very limited sequence homologies (2); however, besides the YD and GXGD domain, a third more C-terminal PAL sequence is conserved among all members of the GXGD proteases (2). Recently it has been shown that the PAL motif may not only present a binding site for transition state inhibitors of γ-secretase and SPP (7), but, at least in the case of PS1, may interact with the N-terminal critical aspartate located within TMD 6 (8, 9). In line with data from electron microscopy (10, 11) and cysteine scanning mutagenesis (12, 13), these findings suggest a water-filled cavity harboring the catalytic center of γ-secretase. For SPP/SPPL family members, no such analyses have been performed yet; therefore it is too early to speculate whether similar structural features as observed for PS1 also apply. Although SPP/SPPLs apparently exert protease function in the absence of additional essential co-factors (1, 14, 15) and can even be functionally expressed in bacteria (16), γ-secretase is a protease complex composed of PS and three additional proteins, Nicastrin (NCT), APH-1 (APH-1a L/S or APH-1b), and PEN-2 (17). All four proteins are necessary and sufficient for authentic γ-secretase function (18). PS harbors the active site aspartyl residues and the interacting PAL motif, whereas NCT is discussed as a substrate receptor (19), and PEN-2 is discussed as a stabilizing factor keeping the auto-proteolytically generated PS fragments in close contact (20, 21). No function has so far been assigned to APH-1.

SPP was discovered as an ICLiP responsible for removing hydrophobic signal peptides liberated from the N terminus of secreted or transmembrane proteins by signal peptidase (SP) cleavage during their co-translocation into the endoplasmic reticulum (1). In addition to signal peptide degradation, SPP is also required for the generation of cell surface histocompatibility antigen-E epitopes and processing of the hepatitis C virus polyprotein (5). A data base search for SPP homologues revealed SPPL2a, b, and c and SPPL3 (2, 3). Currently, little is

known about the function of SPPL family members. No physiological substrates are known for SPPL3 and SPPL2c. In contrast, three substrates have been identified to be processed by SPPL2a/b. These include tumor necrosis factor α (14, 22), the Fas ligand (FasL) (23), and Bri2 (Itm2b) (24). In the case of tumor necrosis factor α, reverse signaling has been observed upon liberation of the intracellular domain (ICD) by SPPL2a and SPPL2b (22). The tumor necrosis factor α ICD regulates expression of interleukin-12 probably via nuclear signaling (22). Similarly, the ICD of FasL negatively regulates gene transcription (23). Consistent with its predominant function in signal peptide removal, SPP is located within the endoplasmic reticulum (15, 22) and probably retained by a KK*XX* retention signal. SPPL3 (15) and SPPL2c (22) are also located within the endoplasmic reticulum, and it is tempting to speculate that they are involved in signal peptide removal like SPP. In contrast, SPPL2a and SPPL2b occur throughout the secretory pathway including the plasma membrane and endosomes/lysosomes (15). This suggests that the differential subcellular localization of SPPL proteases restricts the number of available substrates. In contrast to γ-secretase, which only accepts type 1 transmembrane proteins as substrates for intramembrane proteolysis (17, 25), all currently known SPP/SPPL substrates are in type 2 orientation (1, 5, 14, 22–24). For γ-secretase and other ICLiPs, it has been shown that intramembrane proteolysis strictly follows a previous ectodomain shedding event. Shedding removes the bulk of the ectodomain and leaves behind a small membrane-retained stub. In the case of γ-secretase, substrates with an ectodomain shorter than ~50 amino acids are preferentially processed (26). Moreover, only pre-shed substrates bind to γ-secretase (27), whereas full-length proteins are most likely not recognized. Substrate recognition via its free N terminus is apparently mediated by NCT through a conserved glutamate residue (19), although this finding has recently been challenged (28). SPP may also require precleavage of its substrate by SP (1, 29); however, even upon mutagenesis of the SP recognition site, some residual intramembrane proteolysis still occurs (29). In line with the possibility that full-length substrates may be cleaved at least to some extent, SPPL2b was shown to co-immunoprecipitate both the truncated substrate and the full-length precursor (14, 24). However, the fact that substantially more full-length protein co-immunoprecipitates with the active SPPL2b protein as compared with the truncated fragment suggested that the latter may be preferentially turned over by intramembrane proteolysis (14, 24). It is also not known whether primary sequences within the TMD or adjacent domains of SPPL2b substrates are critical for substrate recognition and turnover.

Bri3 as well as Bri2, which is genetically associated with Familial British and Danish dementia, belong to the family of highly homologous Bri proteins (30). We demonstrate that, although very homologous to Bri2, Bri3 is not a substrate for regulated intramembrane proteolysis. This finding allowed us to study intramembrane proteolysis independent of ectodomain shedding. We demonstrate that shedding greatly facilitates subsequent intramembrane proteolysis. However, truncation of the ectodomain of a potential SPPL2b substrate is surprisingly not sufficient to allow intramembrane proteolysis,

TABLE 1
Generation of chimeric Bri variants and deletions
The numbers represent the corresponding amino acids of Bri2 and Bri3, respectively.

Construct	ICD	TMD	Ectodomain
Bri2	Bri2 1–54	Bri2 55–75	Bri2 76–237
Bri3	Bri3 1–54	Bri3 55–75	Bri3 76–233
Bri2ΔE	Bri2 1–54	Bri2 55–75	Bri2 76–98
Bri3ΔE	Bri3 1–54	Bri3 55–75	Bri3 76–98
Bri2/3	Bri2 1–54	Bri2 55–75	Bri3 76–233
Bri2/3 - 0	Bri2 1–54	Bri2 55–75	
Bri2/3 - 10	Bri2 1–54	Bri2 55–75	Bri3 76–86
Bri2/3 - 23	Bri2 1–54	Bri2 55–75	Bri3 76–98
Bri2/3 - 59	Bri2 1–54	Bri2 55–75	Bri3 76–134
Bri2/3 - 91	Bri2 1–54	Bri2 55–75	Bri3 76–166
Bri2/3 - 124	Bri2 1–54	Bri2 55–75	Bri3 76–199
Bri2/3 - 156	Bri2 1–54	Bri2 55–75	Bri3 76–233
Bri2/3ΔE	Bri2 1–54	Bri2 55–75	Bri3 76–98
Bri3/2/2	Bri3 1–54	Bri2 55–75	Bri2 76–237
Bri2$_{Ins Bri3 45–54}$	Bri2 1–44, Bri3 45–54	Bri2 55–75	Bri2 76–237
Bri2/3/2	Bri2 1–54	Bri3 55–75	Bri2 76–237

because in addition to removal of the bulk of the ectodomain, sequence determinants within the ICD, the TMD, and the luminal juxtamembrane domain (JMD) are also required.

EXPERIMENTAL PROCEDURES

Cell Culture, cDNAs, and Transfection—HEK-293EBNA (HEK-293) were cultured in Dulbecco's modified Eagle's medium with Glutamax (Invitrogen) supplemented with 10% fetal calf serum (Invitrogen) and 1% penicillin/streptomycin (Invitrogen). HEK-293 single cell clones stably expressing SPPL2b or SPPL2b D421A containing a C-terminal hemagglutinin tag (AYPYDVPDYA) have been described before (24). Bri2 and Bri3 cDNAs were purchased from Deutsches Ressourcezentrum für Genomforschung (Berlin, Germany). cDNAs encoding chimeric proteins (Table 1) were generated by PCR. For all constructs the propetide at the C terminus was removed, and a N-terminal FLAG tag (DYKDDDDK) as well as a C-terminal V5 tag (GKPIPNPLLGLDST) was added. Sequences of the oligonucleotides used for PCR are available upon request. PCR products were subcloned into the HindIII and XbaI sites of pcDNA6.0-V5-His A (Invitrogen). All of the cDNA constructs were verified by sequencing. Transient transfection of HEK-293 cell lines stably expressing the indicated SPPL2b variants was carried out using Lipofectamine 2000 (Invitrogen) according to the manufacturer's instructions. The bovine ADAM-10 wt and ADAM-10 E384A constructs are a generous gift from Dr. Rolf Postina.

Antibodies, Immunoprecipitation, and Immunoblotting—The monoclonal anti-FLAG M2 and the polyclonal hemagglutinin 6908 antibody were obtained from Sigma; the poly- and monoclonal V5 antibodies were purchased from Chemicon (Schwalbach, Germany) and Invitrogen, respectively. The polyclonal antibodies against ADAM-10 and calnexin were purchased from Calbiochem and Stressgene/Biomol (Hamburg, Germany). The monoclonal anti-Giantin antibody (ALX-804–600) was obtained from Alexa (AXXORA Deutschland GmbH, Lörach, Germany). 22C11 antibody recognizing the N terminus of APP was purchased from Chemicon (Schwalbach, Germany). Anti-mouse and anti-rabbit secondary antibodies were purchased from Promega (Madison, WI). Immunoprecipitation assays, gel electrophoresis, immunoblotting experi-

ments, and assays were carried out as described previously (14, 15).

Immunocytochemistry and Confocal Imaging—The indicated cell lines were grown on polylysine-coated glass coverslips to 60–80% confluence and processed for immunofluorescence as described before (15). Cells were treated with 0.1% Triton to perform co-staining with the Golgi marker giantin or were left untreated to perform surface stainings. Confocal images were obtained with Zeiss 510Meta confocal laser scanning microscope system equipped with a 100/1.3 objective described previously (31). The images were assembled and processed using Adobe Illustrator.

Inhibitor Treatment and Quantification—To inhibit SPPL2b, the cells were treated overnight with a final concentration of 30 μM (Z-LL)$_2$-ketone (Calbiochem), a known SPP/SPPL inhibitor (32). For quantification, the proteins were immunoblotted as described above and detected using the enhanced chemiluminescence technique (GE Healthcare). The chemiluminescence signals of at least three independent experiments were measured with a CD camera-based imaging system (Alpha Innotec). Statistical significance was determined with Student's t test. Statistical significant p values <0.05, <0.005, and <0.0005 are represented by *, **, and ***, respectively.

Alignment and Sequence Analysis—Bri2 and Bri3 protein sequences were aligned using VectorNTI 9 (Invitrogen). Amino acid identity and similarity were calculated using EMBOSS pairwise alignment algorithms.

RESULTS

Differential Shedding of Bri2 and Bri3—Although substrate requirements for γ-secretase (Ref. 26; summarized in Refs. 17 and 33) and SPP (29) are at least partially described, very little is known about determinants that allow SPPLs to recognize their appropriate protein substrates. Therefore we specifically searched for substrate requirements of SPPL2b, an ICLiP of the GXGD-type located within the late secretory compartments including plasma membrane and endosomes, because this may allow a direct comparison of the properties of γ-secretase with those of the SPPLs. Recently we and others have identified three substrates, tumor necrosis factor α (14, 22), Bri2 (24), and the FasL (23), for intramembrane proteolysis by SPPL2a/b. We now compared the processing of two homologous Bri proteins, Bri2 and Bri3 (30, 34) (Fig. 1*A*). cDNAs encoding the Bri2 or the Bri3 protein were transfected into HEK-293 cell lines stably expressing either wt SPPL2b or the functional inactive SPPL2b D/A (15) mutant. As described previously (24), the BRICHOS domain was efficiently shed upon transfection of Bri2 (Fig. 1*B*). Shedding occurred independent of the expression of wt SPPL2b or nonfunctional SPPL2b D/A. As expected, we also detected the Bri2 N-terminal fragment (Bri2 NTF) generated by the shedding event within the cell lysate (Fig. 1*B*). As observed before (24), the shedding event appeared to be heterogeneous because multiple NTFs of slightly different molecular weight are detected. The Bri2 ICD was efficiently generated upon co-expression of the proteolytically active SPPL2b (Fig. 1*B*). In contrast, upon expression of the inactive SPPL2 D/A variant, the Bri2 NTF accumulated, and no Bri2 ICD was generated (Fig. 1*B*) (24). Interestingly, when we expressed the homologous

Bri3, no secretion of the Bri3 BRICHOS domain was observed (Fig. 1*B*). This is in line with previous findings that also suggested that Bri3 fails to undergo shedding (35). Intramembrane proteolysis by SPPL2b was also not observed, as shown by the lack of detectable Bri3 ICD even after long exposure (Fig. 1*B*). This suggests that although Bri2 and Bri3 share substantial sequence similarities throughout their ectodomains (Fig. 1*A*), the shedding protease discriminates between these similar substrates. However, another possibility would be that Bri2 and Bri3 are differentially targeted and Bri3 does not reach sheddase/SPPL2b containing cellular compartments. To prove this possibility, we investigated the subcellular distribution of Bri2 and Bri3 by immunohistochemistry. This revealed that both Bri2 and Bri3 are similarly targeted through the secretory pathway and occur within giantin-positive Golgi compartments and on the plasma membrane (Fig. 1*C*), and thus both co-localize with SPPL2b (24). From these experiments we conclude that Bri3, although it is quite homologous to Bri2 and occurs within the same subcellular compartments, fails to undergo shedding as well as intramembrane proteolysis.

Ectodomain Shedding Is Not Sufficient for Intramembrane Proteolysis—In line with data obtained for substrate requirements of γ-secretase (26), we postulated that Bri2 and Bri3 variants lacking large parts of their ectodomains may allow efficient intramembrane proteolysis. We therefore generated Bri2 and Bri3 variants lacking almost the entire ectodomain (Bri2ΔE and Bri3ΔE). Upon co-expression with SPPL2b, Bri2ΔE underwent intramembrane proteolysis and allowed production of robust levels of the Bri2 ICD (Fig. 2*A* (24)). The Bri2 ICD was not generated upon treatment with the SPPL2b inhibitor (Z-LL)$_2$-ketone as expected (Fig. 2*A*) (24). Surprisingly, when we expressed Bri3ΔE, no intramembrane proteolysis was detectable (Fig. 2*A*), although the ectodomain should have been sufficiently truncated to allow constitutive intramembrane proteolysis independent of a previous shedding event. This suggests that intramembrane proteolysis may occur only to a very limited level, which, however, is beyond the detection limit for the Bri3 ICD. From these findings we conclude that shedding *per se* is not sufficient to allow constitutive intramembrane proteolysis. Therefore, sequence elements within the small NTF of SPPL2b substrates are additionally required to trigger intramembrane proteolysis. To further pursue the influence of ectodomain shedding on SPPL2b-dependent intramembrane proteolysis, we generated a cDNA construct encoding a Bri variant containing the Bri2 ICD and TMD fused to the Bri3 ectodomain (Bri2/3; Fig. 2*B*). This variant was expressed in HEK-293 cells together with wt SPPL2b or the nonfunctional SPPL2b D/A. Upon expression of Bri2/3, no shedding was detected (Fig. 2*B* and supplemental Fig. S1), confirming again that Bri2 and Bri3 are differentially processed within their ectodomain. Differential targeting of Bri2/3 was excluded, because this chimeric variant is observed throughout the secretory pathway, including a giantin-positive Golgi compartment and the plasma membrane (Fig. 2*C*). Surprisingly, although no shedding occurs as monitored by the lack of the NTF in the cell lysate and the BRICHOS domain in the conditioned medium, SPPL2b-dependent ICD generation was observed to some extent (Fig. 2*B*). It should be noted, however, that ICD genera-
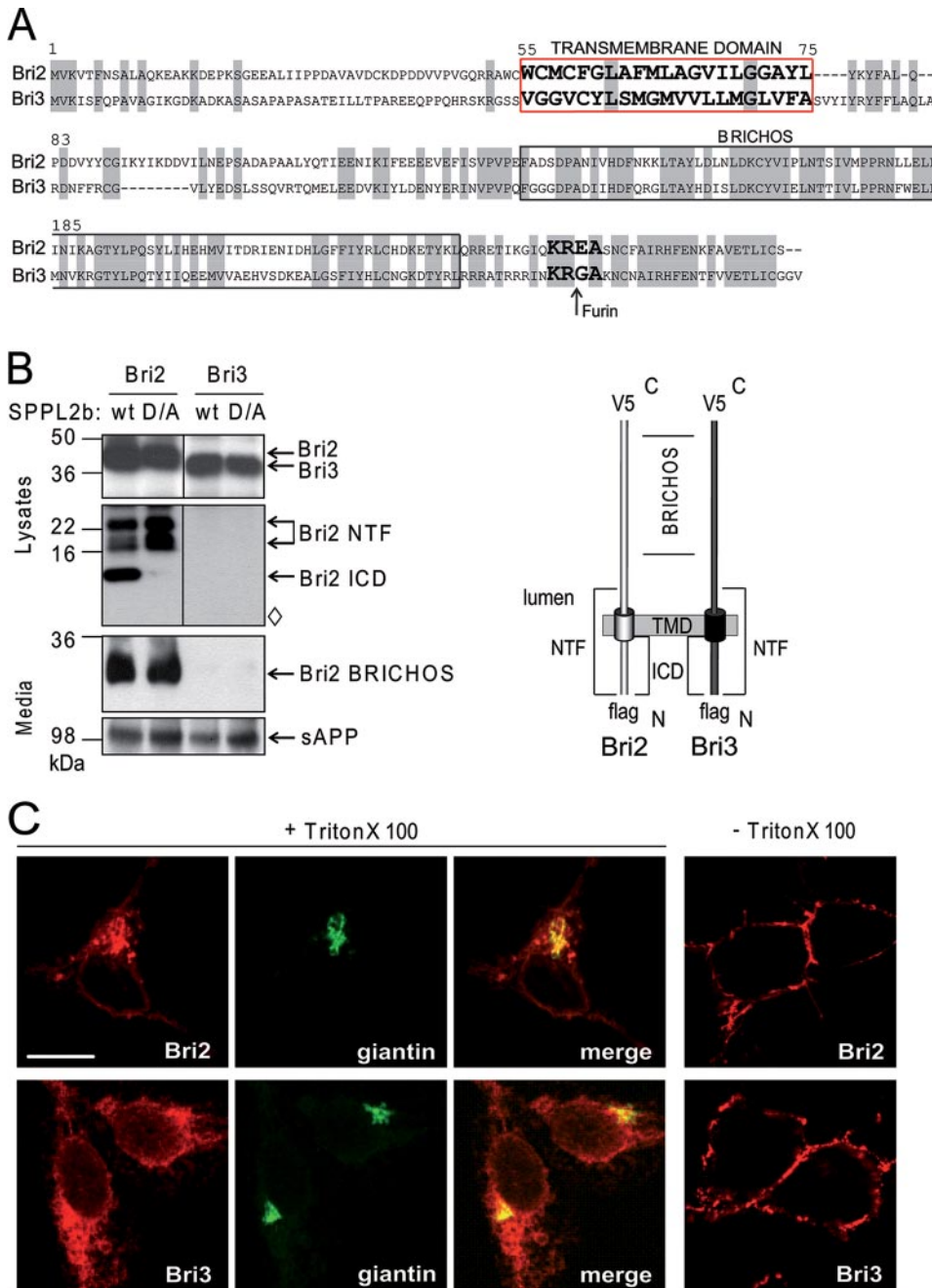
FIGURE 1. **The Bri2 homologue Bri3 is not a substrate for regulated intramembrane proteolysis by SPPL2b.** *A*, amino acid sequence alignment of Bri2 and Bri3. The Furin cleavage site and the transmembrane domain are shown in *bold*, and identical residues are highlighted in *gray*. Sequence identity and similarity are 43 and 60%, respectively. *B*, Bri3 neither undergoes ectodomain shedding nor intramembrane proteolysis by SPPL2b. Upon co-expression of SPPL2b with Bri2 or Bri3 in HEK-293 cells, NTF and ICD generation are observed only for Bri2. Note that Bri2 ICD generation is abolished upon co-expression of the catalytic inactive SPPL2b D/A mutant. The soluble ectodomain (BRICHOS) in conditioned medium is detected for Bri2, but not for Bri3 expressing cells. Full-length Bri as well as the NTFs and ICDs were detected using the anti-FLAG antibody. The corresponding BRICHOS domains were visualized with an anti-V5 antibody. Reprobing for soluble APP with 22C11 antibody shows that ectodomain shedding in general is not affected upon expression of Bri3. The expression levels of SPPL2b were similar in Bri2/Bri3 expressing cells (data not shown). ◇ indicates longer blot exposure. *C*, Bri3 is present in late secretory compartments. Immunohistochemistry of HEK-293 cells transfected with Bri3 reveals localization at the plasma membrane (stainings without Triton X-100) as well as co-localization with the Golgi compartment marker giantin (stainings with Triton X-100). Bri2 and Bri3 were detected using the anti-V5 antibody. The localization of Bri3 and Bri2 is similar. The *scale bar* represents 10 μm.

tion of Bri2/3 was substantially lower as compared with wt Bri2 (Fig. 2*B*). Taken together these findings indicate that shedding facilitates intramembrane proteolysis but is not absolutely required for ICD generation.

Shedding by ADAM-10 Facilitates Intramembrane Proteolysis—To further confirm that shedding facilitates intramembrane proteolysis of a natural substrate, we co-expressed ADAM-10, the major sheddase known to process Bri2 (24), or its catalytically inactive variant ADAM-10 E384A (36) with wt Bri2 and SPPL2b. Enhanced expression of wt ADAM-10 results in elevated levels of the Bri2 NTF in the cell lysate and BRICHOS in the conditioned media, respectively (Fig. 3). Moreover, elevation of shedding caused enhanced ICD generation (Fig. 3), demonstrating that shedding indeed facilitates subsequent intramembrane proteolysis. To further prove this hypothesis, we compared intramembrane proteolysis of full-length Bri2 and Bri2ΔE. In line with the finding that shedding is a rate-limiting step, Bri2ΔE is more efficiently endoproteolyzed by SPPL2b than the full-length protein (data not shown).

Intramembrane Proteolysis Negatively Correlates with the Size of the Ectodomain—A size-selecting mechanism is known as a key step in substrate recognition by γ-secretase. Here the appropriately truncated substrate is apparently identified by NCT (19), and substrates with ectodomains smaller than 50 amino acids are preferentially processed (26). However, in the absence of NCT, no such mechanisms would be expected for SPPL2b, although, surprisingly, we observed that shedding facilitates subsequent intramembrane proteolysis. This may indeed suggest a size-selecting mechanism similar to that reported for γ-secretase. We therefore generated fusion proteins of the Bri2 ICD and TMD with Bri3 ectodomains of increasing length (Fig. 4*A*). This strategy allowed us to investigate whether there is a size selecting process, because the Bri3 ectodomain does not allow shedding (Fig. 1*B*). Surprisingly, we found a strong negative correlation of ICD generation with the size of the ectodomain (Fig. 4, *B* and *C*). Substantial ICD production was observed only upon expression of substrates with less than 59 amino acids in their ectodomain. Most efficient intramem-
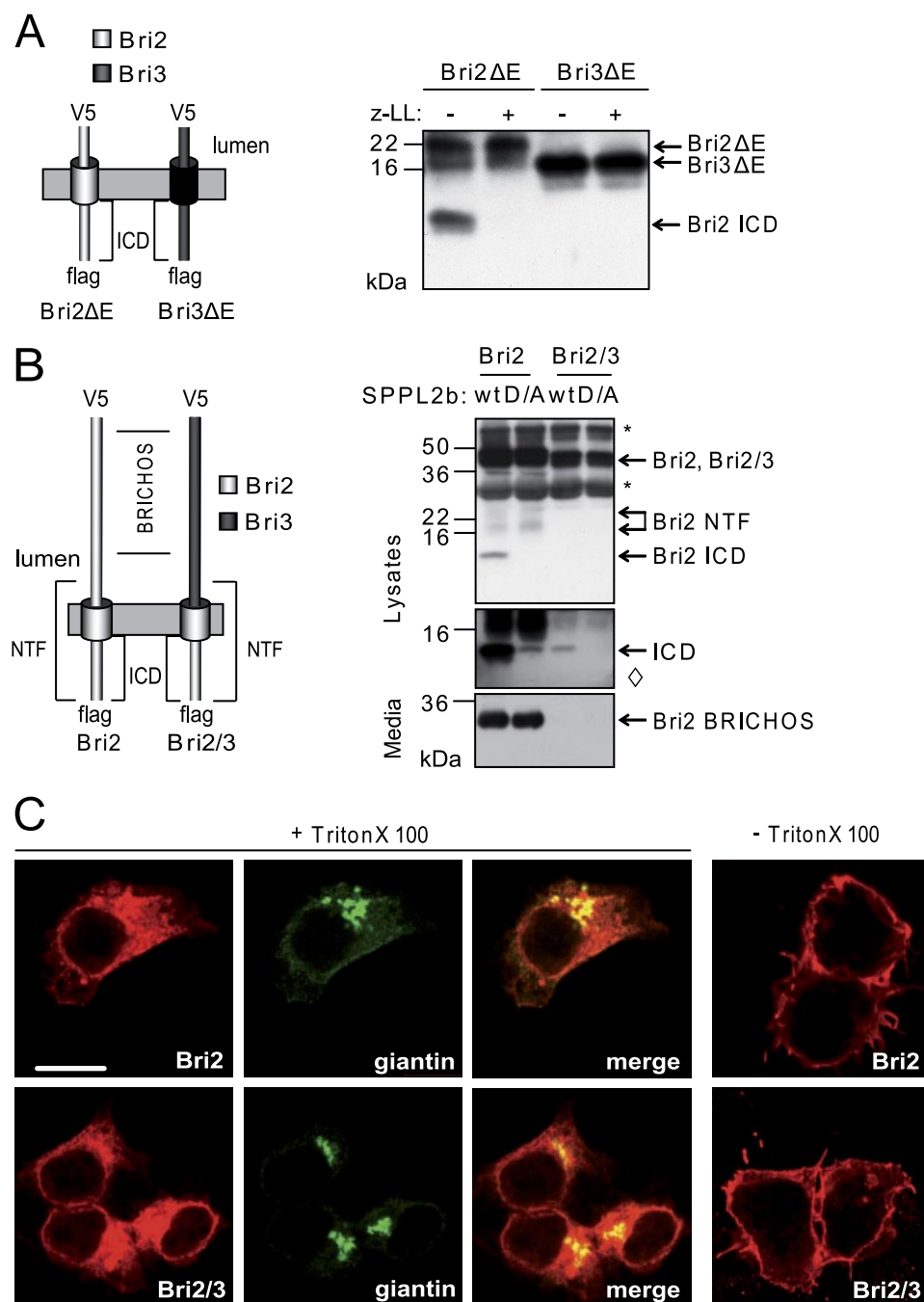
FIGURE 2. **Influence of ectodomain shedding on SPPL2b-dependent intramembrane proteolysis.**
A, shedding per se is not sufficient for SPPL2b-dependent intramembrane proteolysis. Co-expression of SPPL2b with Bri2 or Bri3 mutants lacking the BRICHOS ectodomain (Bri2ΔE or Bri3ΔE) in HEK-293 cells allows SPPL2b-dependent ICD generation for Bri2. Bri2ΔE and Bri3ΔE were detected using the anti-FLAG antibody. Treatment with (Z-LL)₂-ketone inhibits Bri2 ICD generation. Bri3ΔE is not processed by SPPL2b. *B,* ectodomain shedding is not a prerequisite for SPPL2b-dependent intramembrane proteolysis. Upon co-expression of Bri2/3 with SPPL2b, both BRICHOS in the conditioned media and NTF in cell lysates are not detected. For detection of full-length Bri2, Bri2/3, or N-terminal processing products an anti-FLAG antibody was used. The corresponding BRICHOS domains were visualized with an anti-V5 antibody. Bri2/3 does not undergo ectodomain shedding. However, note that low amounts of ICD are generated in a SPPL2b-dependent manner. The remaining Bri2 ICD derived from wt Bri2 upon expression of the nonfunctional D/A SPPL2b mutant is most likely caused by a low level expression of endogenous SPPL2b. *Asterisks* indicate IP antibody cross-reaction, ◇ indicates longer blot exposure. *C,* Bri2/3 is transported to late secretory compartments. Immunohistochemistry of HEK-293 cells transfected with Bri2/3 reveals localization at the plasma membrane (stainings without Triton X-100) as well as co-localization with the Golgi compartment marker giantin (stainings with Triton X-100). Bri2 and Bri2/3 were detected using an anti-V5 antibody. The localization of Bri2 and Bri2/3 is similar. The *scale bar* represents 10 μm.

brane proteolysis occurred with substrates having less than 23 luminal amino acids (Fig. 4, *B* and *C*), which is surprisingly similar to findings made with γ-secretase substrates (26).

Sequence Determinants in All Three Subdomains of the Bri2 NTF Are Required for Intramembrane Proteolysis—The results shown above suggest that in addition to a size selection mechanism, sequence determinants within the NTF of the substrate must also influence SPPL2b cleavage efficiency, because ectodomain truncation of Bri3 is not sufficient to convert Bri3 into a SPPL2b substrate (Fig. 2*A*). Therefore, we first investigated the influence of the luminal JMD on intramembrane proteolysis. We generated Bri ΔE constructs that contained 23 amino acids of the luminal domain of either Bri2 or Bri3 fused to the TMD and ICD of Bri2 (Bri2ΔE and Bri2/3ΔE; Fig. 5*A*) and directly compared the efficiency of SPPL2b-dependent intramembrane proteolysis. This revealed that Bri2/3ΔE is turned over with ~70% less efficiency compared with Bri2ΔE (Fig. 5, *B* and *C*). This is reflected not only by a significant reduction of ICD formation but also by a lack of substrate accumulation upon expression of the nonfunctional SPPL2b D/A mutant (Fig. 5*B*). Thus the luminal 23 amino acid JMD of Bri2 contributes important determinants required for SPPL2b-dependent cleavage.

We next investigated whether the ICD also contributes to intramembrane proteolysis. To do so we fused the Bri3 ICD to the TMD and ectodomain of Bri2, creating Bri3/2/2 (Fig. 6*A*). Expression of Bri3/2/2 revealed about 60% less ICD generation compared with that from the wt Bri2 (Fig. 6, *B* and *C*). This suggests that sequences within the ICD influence intramembrane proteolysis by SPPL2b. To further map the sequence requirements within the cytoplasmic tail, we inserted 10 amino acids of the Bri3 cytosolic juxtamembrane domain into the Bri2 ICD creating Bri2$_{Ins\ Bri3\ 45-54}$ (Fig. 6*D*).
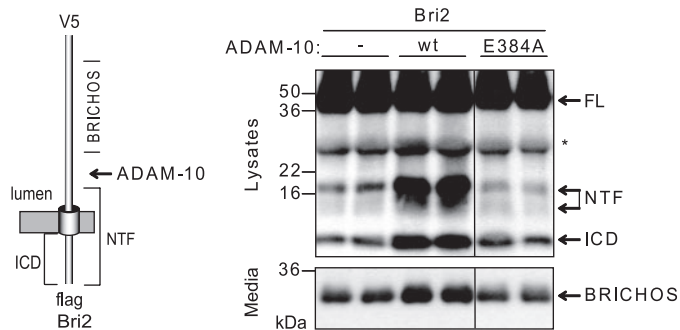
FIGURE 3. Ectodomain shedding facilitates intramembrane proteolysis. ADAM-10 enhances SPPL2b-dependent intramembrane proteolysis. Co-expression of Bri2 with wt ADAM-10, but not with the inactive E384A ADAM-10 mutant in HEK-293 cells, leads to increased amount of NTF in cell lysates and BRICHOS secretion into the conditioned medium. Bri2 and its N-terminal processing products were detected using an anti-FLAG antibody. The corresponding BRICHOS domain was visualized with an anti-V5 antibody. ICD levels are increased in cells expressing wt ADAM-10, showing that ectodomain shedding facilitates SPPL2b-dependent intramembrane proteolysis. The *asterisk* indicates IP antibody cross-reaction.

Expression of $Bri2_{Ins\ Bri3\ 45-54}$ revealed an ~60% reduction of ICD formation (Fig. 6, *E* and *F*) very similar to the reduced intramembrane proteolysis upon expression of Bri3/2/2 (Fig. 6, *B* and *C*). Thus it is likely that the 10 amino acids of the juxtamembrane domain immediately beyond the membrane play a major role for substrate recognition.

The above-described experiments (Fig. 2*A*) suggest that the TMD may also be important for subsequent intramembrane proteolysis, because the Bri2/3 variant allowed at least some intramembrane proteolysis, whereas Bri3ΔE failed to undergo cleavage by SPPL2b (Fig. 2*A*). To further support this hypothesis, we replaced the TMD of Bri2 by that of Bri3, generating the Bri2/3/2 variant (Fig. 7*A*). Bri2 and Bri2/3/2 were expressed with SPPL2b in HEK-293 cells. Substantial amounts of Bri2 ICD were generated from wt Bri2 as expected (Fig. 7*B*). However, upon expression of Bri2/3/2, we observed an ~80% reduction of ICD formation (Fig. 7, *B* and *C*). This suggests that, in addition to the luminal JMD and the ICD, the TMD of Bri2 also provides very important sequence determinants.

DISCUSSION

Intramembrane proteolysis is becoming an increasingly important cellular mechanism involved in numerous signaling pathways as well as in protein degradation. Furthermore, some of these proteases such as γ-secretase are major players in abundant diseases, including Alzheimer disease. γ-Secretase together with SPP and the SPPLs represent the currently known eukaryotic GXGD-type aspartyl proteases. We have now investigated the substrate requirements of SPPL2b. As described above, SPPL2b, like the other members of the SPP/SPPL family, does not require additional co-factors for activity like γ-secretase. We therefore expected that SPPL2b may have some fundamentally different substrate requirements as compared with γ-secretase. For example, one would have expected that SPPL2b may not depend on trimming of its substrates by shedding, because a size-selecting substrate receptor like NCT is not required, and SPPL2a and SPPL2b are biologically active on their own (14, 15, 22–24). Surprisingly, we found some substantial similarities in substrate selection of
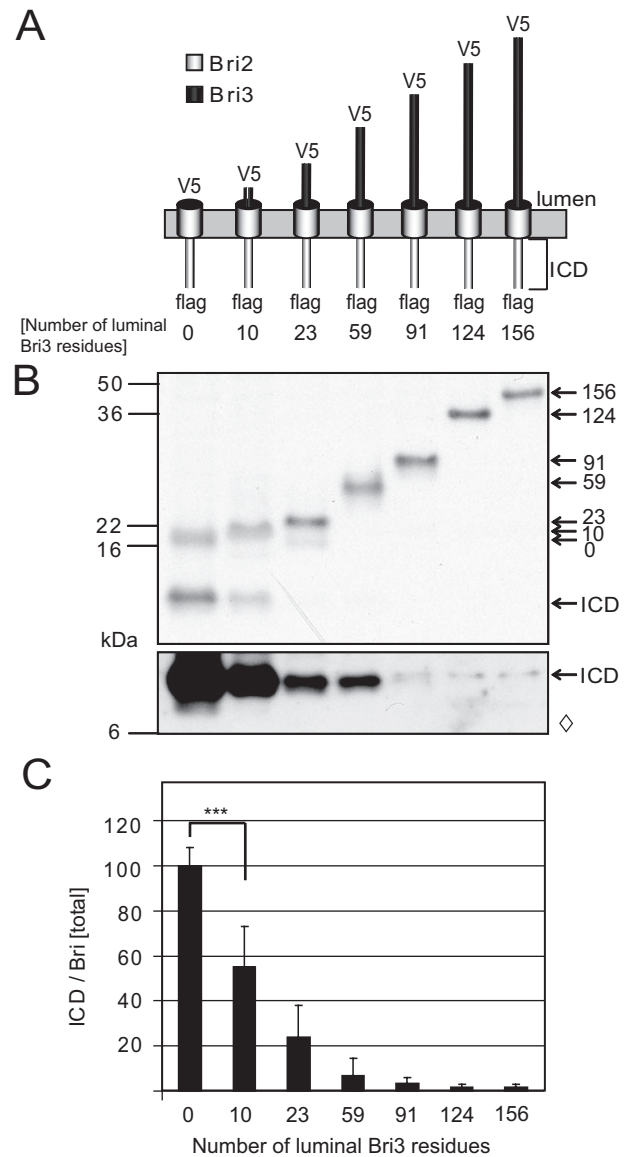

FIGURE 4. Intramembrane proteolysis negatively correlates with the size of the ectodomain. *A*, model of the Bri2/3 fusion proteins. All constructs contain the ICD and the TMD of Bri2 but contain increasing parts of the Bri3 luminal domain. *B*, a short luminal domain of the substrate increases SPPL2b cleavage efficiency. HEK-293 cells stably expressing SPPL2b were transfected with the Bri2/3 fusion constructs shown in *A*. All fusion proteins were detected using an anti-FLAG antibody. Robust generation of ICD is observed only for the two shortest constructs (none or 10 luminal Bri3 residues). Increasing the size of the luminal domain leads to decreased amounts of ICD. ◇ indicates longer blot exposure. *C*, quantitative analysis of experiment shown in *B*. The data represent the means ± S.D. of nine independent experiments. The relative signal intensity of ICD compared with full-length protein was measured for each construct, normalized to calnexin, and set to 100% for the shortest construct. The addition of 10 luminal Bri3 residues to the shortest construct leads to a 45% decrease in SPPL2b-dependent cleavage efficiency ($p = 0.00009$). Increasing the length of the luminal domain further reduces the amount of ICD.

γ-secretase and SPPL2b. Clearly, SPPL2b-mediated endoproteolysis is greatly facilitated by previous shedding of the ectodomain of the substrate. In line with this notion, intramembrane proteolysis by SPPL2b is enhanced by expression of ADAM-10, the major Bri2 cleaving sheddase, or by sequentially truncating the ectodomain of the substrate. Very similar to γ-secretase, which only efficiently
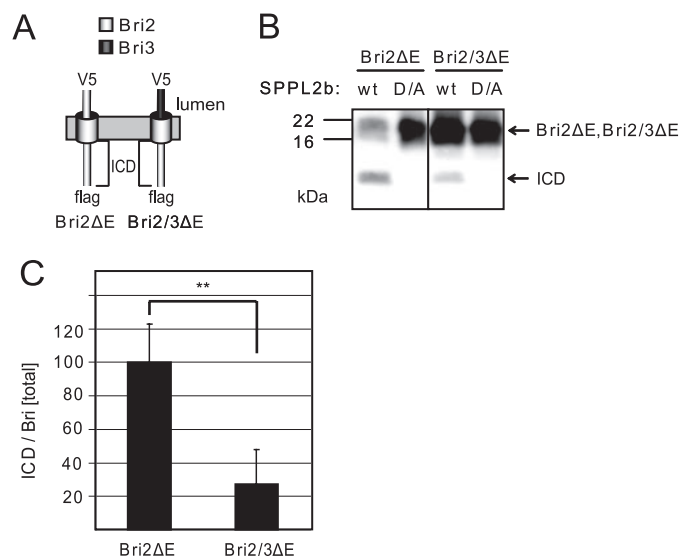
FIGURE 5. **The luminal JMD contributes to substrate recognition for intramembrane proteolysis by SPPL2b.** *A*, model of the chimeric Bri2/3ΔE variant. Only the luminal JMD of Bri2 is replaced by Bri3. *B*, Bri2/3ΔE is less efficiently processed by SPPL2b. Co-expression of Bri2/3ΔE with SPPL2b or SPPL2b D/A reveals reduced SPPL2b-dependent ICD generation compared with co-expression with Bri2ΔE. Chimeric Bri constructs were detected using an anti-FLAG antibody. *C*, quantitative analysis of experiment shown in *B*. The data represent the means ± S.D. of nine independent experiments. The relative signal intensity of ICD compared with full-length protein was measured, normalized to calnexin, and set to 100% for Bri2ΔE. SPPL2b-dependent ICD generation for Bri2/3ΔE is reduced to 27% compared with Bri2ΔE ($p = 0.0007$).

processes substrates with an ectodomain smaller than 50 amino acids (26), SPPL2b-mediated cleavage is more efficient the shorter the ectodomain is. Even the preferred size of the ectodomain is similar for SPPL2b and γ-secretase (26). However, the size of the ectodomain is an important, but not exclusive, determinant for a SPPL2b substrate. This is rather surprising, because SPPL2b does not interact with a NCT-like protein, which could serve as a substrate receptor and size selector. This raises the question of whether a domain within SPPL2b itself could mediate substrate selection. The only domains that may protrude into the luminal space could be the hydrophilic loop between TMD 6 and TMD 7 and the N-terminal domain of SPPL2b. The N-terminal domain prior to TMD 1 is likely to be functionally irrelevant, because SPP itself functions in the absence of its N-terminal domain (16). The hydrophilic loop between TMD 6 and TMD 7 is rather short and not well conserved, suggesting that it is probably not suitable as a substrate receptor for GXGD-aspartyl proteases. However, although the model that NCT serves as the size-selecting substrate acceptor is very attractive, more recently it has been shown that a critical glutamate thought to directly interact via a salt bridge with the free N terminus of the shedded substrate could be mutagenized to glutamine without significantly affecting γ-secretase activity (28). Thus NCT may not be the substrate selecting subunit within the γ-secretase complex. Based on the similar substrate requirements in terms of the length of the ectodomain of γ-secretase and SPPL2b, one may argue that PS itself could also harbor both a substrate binding site and the size selector.
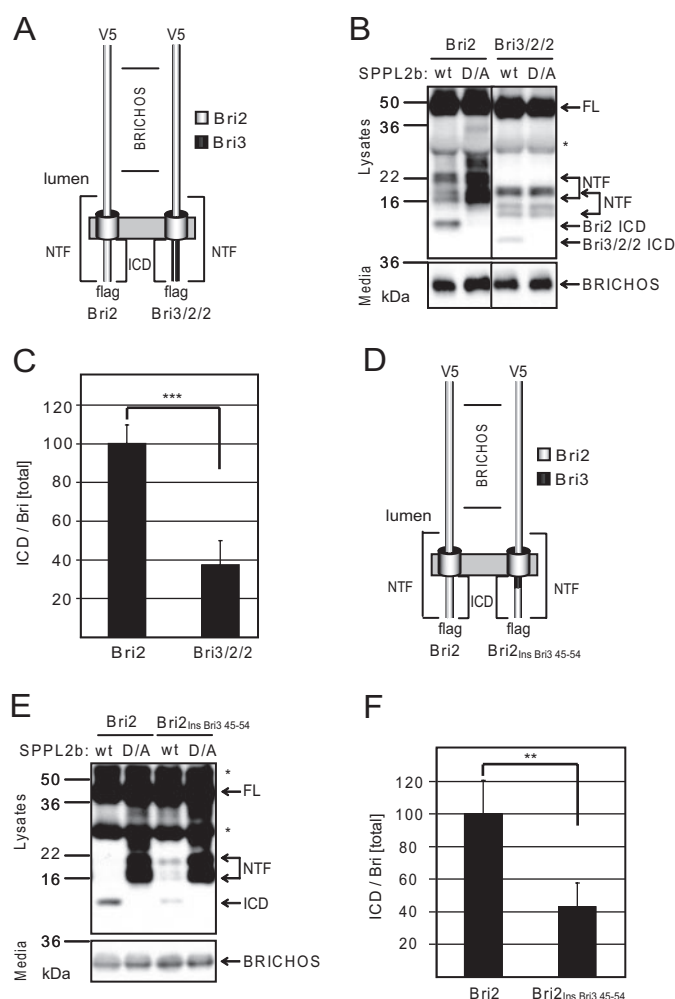

FIGURE 6. **The intracellular domain contributes to substrate recognition for intramembrane proteolysis by SPPL2b.** *A*, model of the chimeric Bri3/2/2 variant. The ICD of Bri2 is replaced by that of Bri3. *B*, Bri3/2/2 is less efficiently processed than Bri2. Co-expression of Bri3/2/2 or Bri2 with SPPL2b or the inactive SPPL2b D/A variant shows reduced ICD generation for Bri3/2/2. Full-length Bri2 and Bri3/2/2 and their N-terminal processing products were detected using the anti-FLAG antibody. The corresponding BRICHOS domains were visualized with an anti-V5 antibody. The Bri3/2/2 NTF and the ICD show an altered running behavior, probably caused by the difference in the ICD sequence. Analysis of conditioned medium shows normal BRICHOS secretion and thus no influence on the ectodomain shedding by the Bri3 ICD. *C*, quantitative analysis of experiment shown in *B*. The data represent the means ± S.D. of eight independent experiments. The relative signal intensity of ICD compared with full-length protein and NTF was measured for both constructs, normalized to calnexin, and set to 100% for Bri2. SPPL2b-dependent ICD generation is reduced to 37% for Bri3/2/2 ($p = 0.000009$). *D*, model of the chimeric Bri2$_{Ins\ Bri3\ 45-54}$ variant. 10 amino acids of the cytosolic juxtamembrane domain of Bri2 have been replaced by those of Bri3. *E*, Bri2$_{Ins\ Bri3\ 45-54}$ is less efficiently processed than Bri2. Co-expression of Bri2$_{Ins\ Bri3\ 45-54}$ or Bri2 with SPPL2b or the inactive SPPL2b D/A variant shows reduced ICD generation for Bri2$_{Ins\ Bri3\ 45-54}$ comparable with Bri3/2/2. Full-length Bri2 and Bri2$_{Ins\ Bri3\ 45-54}$, and their N-terminal processing products were detected using the anti-FLAG antibody. The corresponding BRICHOS domains were visualized with an anti-V5 antibody. Analysis of conditioned media shows normal BRICHOS secretion and thus no influence on the ectodomain shedding by the Bri3 juxtamembrane domain. *F*, quantitative analysis of experiment shown in *E*. The data represent the means ± S.D. of six independent experiments. The relative signal intensity of ICD compared with full-length protein and NTF was measured for both constructs, normalized to calnexin and set to 100% for Bri2. SPPL2b-dependent ICD generation is reduced to 43% for Bri2$_{Ins\ Bri3\ 45-54}$ ($p = 0.00154$).

Although shedding greatly facilitates subsequent intramembrane proteolysis, it is by itself not sufficient for SPPL2b-mediated endoproteolysis. This is reflected by the facts that (i)
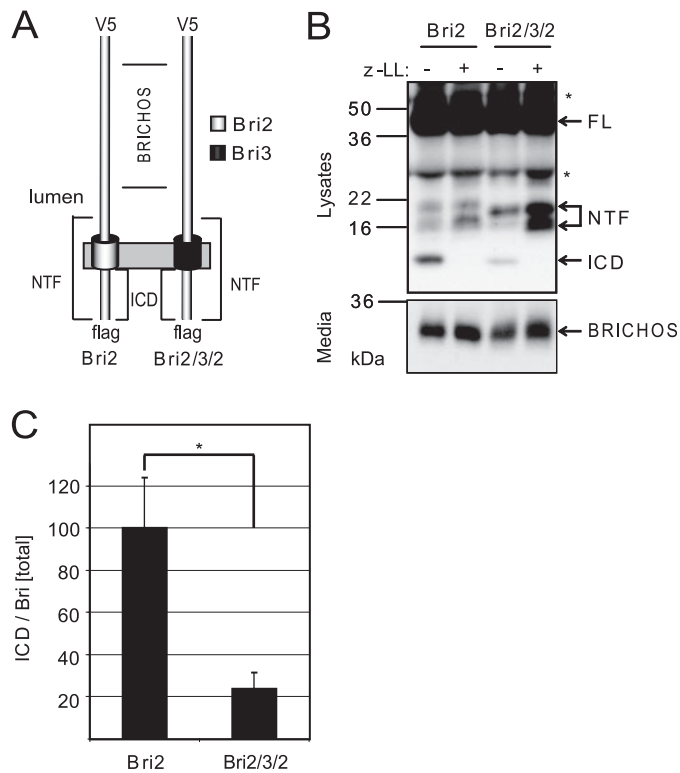
FIGURE 7. **The transmembrane domain sequence is critical for SPPL2b-dependent intramembrane proteolysis.** *A,* model of the chimeric Bri2/3/2 variant. The TMD of Bri2 is replaced by Bri3. *B, Bri2/3/2 is less efficiently processed than Bri2.* Co-expression of Bri2/3/2 or Bri2 with SPPL2b or the inactive SPPL2b D/A variant shows a reduction in ICD formation for Bri2/3/2. Full-length Bri2 and Bri2/3/2 and their N-terminal processing products were detected using the anti-FLAG antibody. The corresponding BRICHOS domains were visualized with an anti-V5 antibody. The Bri2/3/2 NTF shows an altered running behavior, probably caused by the difference in the TMD sequence. The apparent molecular weight of the Bri2/3/2 ICD is similar to that of Bri2. Analysis of conditioned medium shows normal BRICHOS secretion and thus no influence on the ectodomain shedding by the Bri3 TMD. *C,* quantitative analysis of experiment shown in *B.* The data represent the means ± S.D. of three independent experiments. The relative signal intensity of ICD compared with full-length protein plus NTF was measured for both constructs, normalized to calnexin, and set to 100% for Bri2. Replacement of Bri2 TMD with Bri3 TMD leads to a reduction of SPPL2b cleavage efficiency to 23% ($p = 0.02$).

Bri3ΔE undergoes inefficient endoproteolysis and (ii) fusing the ICD and TMD of Bri2 to the ectodomain of Bri3 allows at least some intramembrane proteolysis, although shedding is prevented.

The TMD provides additional substrate requirements that are important for SPPL2b-mediated intramembrane proteolysis. This may be in contrast to γ-secretase, where so far it appears that numerous C-terminal fragments upon removal of their ectodomains are substrates for the "membrane proteasome function" of γ-secretase (37). On the other hand, phenylalanine scanning of the TMD of the β-amyloid precursor protein (APP) revealed at least some sequence specificity for γ-secretase (38). This is also supported by a mutagenesis analysis of the *GXGD* domain within PS1, which suggests at least some substrate specificity of PS1 itself (39). For SPP, it has been described that the TMD requires helix-breaking residues to allow intramembrane cleavage (29). However, the TMD of Bri3 also contains multiple helix-braking residues but fails to be processed efficiently by SPPL2b even upon removal of the Bri3

ectodomain. In line with this finding, intramembrane cleavage still took place at least to some extent upon mutagenesis of the helix-breaking residue within a SPP substrate (29). A very recent study also suggests that amino acids not having a helix breaking potential critically influence intramembrane proteolysis by SPP (40). In addition to the TMD, we found that both the luminal 23 amino acid of the JMD and the ICD also contribute to the cleavability of Bri2. This is in line with the recent observation that the JMD of APP is also required for efficient γ-secretase-mediated proteolysis (41). Furthermore, Hemming *et al.* (42) recently described substrate requirements for γ-secretase substrates. Similar to the substrate requirements for SPPL2b, they found that not only shedding of the ectodomain but also a permissive transmembrane and cytoplasmic domain is required. Moreover, in this study a very restricted substrate selection was observed, which also challenges the idea that γ-secretase functions like a membrane proteasome (37).

Interestingly, the very homologous Bri2 and Bri3 proteins differ dramatically in terms of shedding. Whereas Bri2 is efficiently shedded, Bri3 fails to be processed efficiently by a shedding activity. This is specifically surprising, because sheddases of the ADAM family exhibit no clear sequence specificity but may rather recognize cleavage sites a short distance from the plasma membrane (43). In that regard it is important to note that both proteins reach the plasma membrane. Thus other determinants such as dimerization and/or tertiary structure may play a role. Indeed, β-secretase, another shedding protease, preferentially processes dimerized APP (44–46).

In conclusion SPPL2b has the following substrate requirements: (i) a significantly truncated ectodomain, (ii) an appropriate TMD, (iii) a suitable JMD, and (iv) an appropriate sequence in the ICD. Only a combination of all these determinants allows efficient intramembrane proteolysis. In addition a type 2 orientation of the substrate may be important, because at least so far no type 1-oriented protein was identified as a SPPL2b substrate.

Based on these findings and the similar substrate requirements of γ-secretase, we propose multiple substrate/enzyme interactions within both juxtamembrane regions and the TMD. This model may be supported by the recent findings that γ-secretase protrudes into the extracellular and to some extent also into the cytoplasmic space (11).

REFERENCES

1. Weihofen, A., Binns, K., Lemberg, M. K., Ashman, K., and Martoglio, B. (2002) *Science* **296,** 2215–2218
2. Ponting, C. P., Hutton, M., Nyborg, A., Baker, M., Jansen, K., and Golde, T. E. (2002) *Hum. Mol. Genet.* **11,** 1037–1044
3. Martoglio, B., and Golde, T. E. (2003) *Hum. Mol. Genet.* **12,** 201–206
4. Haass, C., and Steiner, H. (2002) *Trends Cell Biol.* **12,** 556–562
5. Weihofen, A., and Martoglio, B. (2003) *Trends Cell Biol.* **13,** 71–78
6. Steiner, H., Kostka, M., Romig, H., Basset, G., Pesold, B., Hardy, J., Capell, A., Meyn, L., Grim, M. G., Baumeister, R., Fechteler, K., and Haass, C.

(2000) *Nat. Cell Biol.* **2,** 848–851

7. Wang, J., Beher, D., Nyborg, A. C., Shearman, M. S., Golde, T. E., and Goate, A. (2006) *J. Neurochem.* **96,** 218–227
8. Tolia, A., Horré, K., and De Strooper, B. (2008) *J. Biol. Chem.* **283,** 19793–19803
9. Sato, C., Takagi, S., Tomita, T., and Iwatsubo, T. (2008) *J. Neurosci.* **28,** 6264–6271
10. Lazarov, V. K., Fraering, P. C., Ye, W., Wolfe, M. S., Selkoe, D. J., and Li, H. (2006) *Proc. Natl. Acad. Sci. U. S. A.* **103,** 6889–6894
11. Osenkowski, P., Li, H., Ye, W., Li, D., Aeschbach, L., Fraering, P. C., Wolfe, M. S., Selkoe, D. J., and Li, H. (2008) *J. Mol. Biol.* **385,** 642–652
12. Tolia, A., Chavez-Gutierrez, L., and De Strooper, B. (2006) *J. Biol. Chem.* **281,** 27633–27642
13. Sato, C., Morohashi, Y., Tomita, T., and Iwatsubo, T. (2006) *J. Neurosci.* **26,** 12081–12088
14. Fluhrer, R., Grammer, G., Israel, L., Condron, M. M., Haffner, C., Friedmann, E., Bohland, C., Imhof, A., Martoglio, B., Teplow, D. B., and Haass, C. (2006) *Nat. Cell Biol.* **8,** 894–896
15. Krawitz, P., Haffner, C., Fluhrer, R., Steiner, H., Schmid, B., and Haass, C. (2005) *J. Biol. Chem.* **280,** 39515–39523
16. Narayanan, S., Sato, T., and Wolfe, M. S. (2007) *J. Biol. Chem.* **282,** 20172–20179
17. Haass, C. (2004) *EMBO J.* **23,** 483–488
18. Edbauer, D., Winkler, E., Regula, J. T., Pesold, B., Steiner, H., and Haass, C. (2003) *Nat. Cell Biol.* **5,** 486–488
19. Shah, S., Lee, S. F., Tabuchi, K., Hao, Y. H., Yu, C., LaPlant, Q., Ball, H., Dann, C. E., 3rd, Sudhof, T., and Yu, G. (2005) *Cell* **122,** 435–447
20. Prokop, S., Shirotani, K., Edbauer, D., Haass, C., and Steiner, H. (2004) *J. Biol. Chem.* **279,** 23255–23261
21. Hasegawa, H., Sanjo, N., Chen, F., Gu, Y. J., Shier, C., Petit, A., Kawarai, T., Katayama, T., Schmidt, S. D., Mathews, P. M., Schmitt-Ulms, G., Fraser, P. E., and St George-Hyslop, P. (2004) *J. Biol. Chem.* **279,** 46455–46463
22. Friedmann, E., Hauben, E., Maylandt, K., Schleeger, S., Vreugde, S., Lichtenthaler, S. F., Kuhn, P. H., Stauffer, D., Rovelli, G., and Martoglio, B. (2006) *Nat. Cell Biol.* **8,** 843–848
23. Kirkin, V., Cahuzac, N., Guardiola-Serrano, F., Huault, S., Luckerath, K., Friedmann, E., Novac, N., Wels, W. S., Martoglio, B., Hueber, A. O., and Zornig, M. (2007) *Cell Death Differ.* **14,** 1678–1687
24. Martin, L., Fluhrer, R., Reiss, K., Kremmer, E., Saftig, P., and Haass, C. (2008) *J. Biol. Chem.* **283,** 1644–1652
25. Steiner, H. (2008) *Curr. Alzheimer Res.* **5,** 147–157
26. Struhl, G., and Adachi, A. (2000) *Mol. Cell* **6,** 625–636
27. Esler, W. P., Kimberly, W. T., Ostaszewski, B. L., Ye, W., Diehl, T. S., Selkoe, D. J., and Wolfe, M. S. (2002) *Proc. Natl. Acad. Sci. U. S. A.* **99,** 2720–2725
28. Chavez-Gutierrez, L., Tolia, A., Maes, E., Li, T., Wong, P. C., and de Strooper, B. (2008) *J. Biol. Chem.* **283,** 20096–20105
29. Lemberg, M. K., and Martoglio, B. (2002) *Mol. Cell* **10,** 735–744
30. Choi, S. C., Kim, J., Kim, T. H., Cho, S. Y., Park, S. S., Kim, K. D., and Lee, S. H. (2001) *Mol. Cell* **12,** 391–397
31. Kaether, C., Capell, A., Edbauer, D., Winkler, E., Novak, B., Steiner, H., and Haass, C. (2004) *EMBO J.* **23,** 4738–4748
32. Weihofen, A., Lemberg, M. K., Ploegh, H. L., Bogyo, M., and Martoglio, B. (2000) *J. Biol. Chem.* **275,** 30951–30956
33. Steiner, H., Fluhrer, R., and Haass, C. (2008) *J. Biol. Chem.* **283,** 29627–29631
34. Pittois, K., Deleersnijder, W., and Merregaert, J. (1998) *Gene* (*Amst.*) **217,** 141–149
35. Wickham, L., Benjannet, S., Marcinkiewicz, E., Chretien, M., and Seidah, N. G. (2005) *J. Neurochem.* **92,** 93–102
36. Lammich, S., Kojro, E., Postina, R., Gilbert, S., Pfeiffer, R., Jasionowski, M., Haass, C., and Fahrenholz, F. (1999) *Proc. Natl. Acad. Sci. U. S. A.* **96,** 3922–3927
37. Kopan, R., and Ilagan, M. X. (2004) *Nat Rev Mol. Cell. Biol.* **5,** 499–504
38. Lichtenthaler, S. F., Wang, R., Grimm, H., Uljon, S. N., Masters, C. L., and Beyreuther, K. (1999) *Proc. Natl. Acad. Sci. U. S. A.* **96,** 3053–3058
39. Yamasaki, A., Eimer, S., Okochi, M., Smialowska, A., Kaether, C., Baumeister, R., Haass, C., and Steiner, H. (2006) *J. Neurosci.* **26,** 3821–3828
40. Okamoto, T., Omori, H., Kaname, Y., Abe, T., Nishimura, Y., Suzuki, T., Miyamura, T., Yoshimori, T., Moriishi, K., and Matsuura, Y. (2008) *J. Virol.* **82,** 3480–3489
41. Ren, Z., Schenk, D., Basi, G. S., and Shapiro, I. P. (2007) *J. Biol. Chem.* **282,** 35350–35360
42. Hemming, M. L., Elias, J. E., Gygi, S. P., and Selkoe, D. J. (2008) *PLoS Biol.* **6,** 2314–2328
43. Sisodia, S. S. (1992) *Proc. Natl. Acad. Sci. U. S. A.* **89,** 6075–6079
44. Kaden, D., Munter, L. M., Joshi, M., Treiber, C., Weise, C., Bethge, T., Voigt, P., Schaefer, M., Beyermann, M., Reif, B., and Multhaup, G. (2008) *J. Biol. Chem.* **283,** 7271–7279
45. Scheuermann, S., Hambsch, B., Hesse, L., Stumm, J., Schmidt, C., Beher, D., Bayer, T. A., Beyreuther, K., and Multhaup, G. (2001) *J. Biol. Chem.* **276,** 33923–33929
46. Munter, L. M., Voigt, P., Harmeier, A., Kaden, D., Gottschalk, K. E., Weise, C., Pipkorn, R., Schaefer, M., Langosch, D., and Multhaup, G. (2007) *EMBO J.* **26,** 1702–1712

Substrate Requirements for SPPL2b-dependent Regulated Intramembrane Proteolysis

Lucas Martin, Regina Fluhrer and Christian Haass

Access the most updated version of this article at doi: 10.1074/jbc.M807485200

Alerts:
- When this article is cited
- When a correction for this article is posted

Click here to choose from all of JBC's e-mail alerts

Supplemental material:
http://www.jbc.org/content/suppl/2008/12/30/M807485200.DC1

This article cites 46 references, 25 of which can be accessed free at
http://www.jbc.org/content/284/9/5662.full.html#ref-list-1